

## Gapped excitation in dense Kondo lattice CePtZn

L. Harriger,<sup>1,\*</sup> S. M. Disseler,<sup>1</sup> J. Gunasekera,<sup>2</sup> J. Rodriguez-Rivera,<sup>1,3</sup> J. Pixley,<sup>4</sup> P. Manfrinetti,<sup>5</sup>  
S. K. Dhar,<sup>6</sup> and D. K. Singh<sup>2,†</sup>

<sup>1</sup>*NIST Center for Neutron Research, Gaithersburg, Maryland 20899, USA*

<sup>2</sup>*Department of Physics and Astronomy, University of Missouri, Columbia, Missouri 65211, USA*

<sup>3</sup>*Department of Materials Sciences, University of Maryland, College Park, Maryland 20742, USA*

<sup>4</sup>*Department of Physics, University of Maryland, College Park, Maryland 20742, USA*

<sup>5</sup>*Department of Chemistry, University of Genova, 16126 Italy*

<sup>6</sup>*DCMPMS, Tata Institute of Fundamental Research, Mumbai 400005, India*

(Received 2 August 2016; published 10 January 2017)

We report on neutron scattering and muon spin relaxation measurements of dense Kondo lattice CePtZn. The system develops long-range incommensurate magnetic order as the temperature is reduced below  $T_N = 1.75$  K. Interestingly, a  $Q$ -independent gap at  $E = 0.65$  meV in the energy spectrum is found to co-exist with the long-range magnetic order. The gap persists to a very high temperature of  $T \simeq 100$  K. The  $Q$ -independent characteristic and its persistence to high temperature hint that the gapped excitation may be manifesting the excited state of the ground-state doublet of the crystal-field energy levels. However, the observed broadness in the linewidth with distinct temperature and field dependencies makes it a nontrivial phenomenon. Qualitative analysis of the experimental data suggests the possible co-existence of a local critical behavior, which is onset near the critical field of  $H \simeq 3$  T, with the crystal-field excitation in the dynamic properties.

DOI: [10.1103/PhysRevB.95.041102](https://doi.org/10.1103/PhysRevB.95.041102)

Kondo lattice systems, typically realized in the intermetallic rare-earth compounds containing a lattice of  $4f$  or  $5f$  electrons (as found in U, Ce, and Yb), tend to exhibit novel dynamic magnetic properties at low temperature that, in some cases, coincide with the unconventional superconductivity [1–3]. The dynamic state often depicts a magnetic quantum critical state (QCP), where the underlying magnetism is controlled by the competing interactions between the single-ion Kondo effect and the long-range Rudermann-Kittel-Kasuya-Yoshida (RKKY) exchange interaction [4–9]. In addition to the quantum critical phase, heavy fermion systems also provide an ideal setup to study interesting properties of magnetic materials in general, such as the coupling between the crystal-field excitation and long-range magnetic order or the presence of gapped excitations in the ordered state. The heavy fermion compounds  $CeMX$ , where  $M = Pd, Pt, Ni$  and  $X = Sn, Zn$ , exhibit a plethora of interesting magnetic properties, namely, successive magnetic phase transitions in CePtSn, quasigap formation due to the valence fluctuation in CeNiSn and incommensurate magnetic reflections suggesting the spin density wave propagation in CePdSn [11–14]. A small subgroup of this family, CePtX, where  $X = Sn, Zn$ , are dense Kondo lattices—a characteristic also reflected in the electronic properties of their Yb analogue, such as YbPtZn [10,15,16]. Among them, CePtZn is an archetypal intermetallic heavy fermion compound.

We have performed detailed neutron scattering and muon spin relaxation ( $\mu$ SR) measurements on a polycrystalline sample of CePtZn. Experimental investigations of CePtZn using neutron scattering and muon spin relaxation have revealed interesting new properties that can have strong implications in understanding the dynamic properties of heavy fermion

systems. It is found that the onset of magnetic order in CePtZn,  $T_N = 1.75$  K, is accompanied by a wave-vector independent gap at  $E = 0.65$  meV in the energy spectrum. The magnetic gap tends to persist to a high temperature of  $T \simeq 100$  K. Interestingly, the gapped excitation is fully suppressed in applied magnetic field in excess of  $H = 8$  T, which is significantly larger than the critical field of  $H_c = 3$  T at which the long-range order disappears. The qualitative analysis of inelastic neutron scattering data indicates the coexistence of a quantum critical state with the crystal-field excitation at  $H > 3$  T. This is consistent with a recent report on the study of CePtZn using electrical and magnetic measurements, which suggested the evolution of a magnetic field tuned quantum critical state near the critical field value [10].

Neutron scattering measurements were performed on a 5.1-g high-quality polycrystalline sample of CePtZn on the spin-polarized triple-axis spectrometer (SPINS) and multi-axis crystal spectrometer (MACS) with fixed final neutron energies of 3.7 and 2.7 meV, respectively. High-resolution measurements on SPINS were performed at the final neutron energy of  $E_f = 2.5$  meV. The high quality of the sample was verified using Guinier-Stoe camera utilizing Cu  $K_\alpha$  radiation and metallographic analysis that confirmed the TiNiSi-type orthorhombic structure of CePtZn [Fig. 1(a)] with lattice parameters of  $a = 7.08 \text{ \AA}$ ,  $b = 4.364 \text{ \AA}$ , and  $c = 8.108 \text{ \AA}$  [10]; also confirmed by the high-resolution neutron scattering measurements [Figs. 1(b) and 1(c)]. Inelastic measurements at SPINS employed a focused pyrolytic graphite (PG) analyzer with a collimator sequence mono-open-sample-BeO-radial colimeter-11 blades focused analyzer-open detector, while the measurements on MACS were performed using a focused PG analyzer and a Be filter utilizing all twenty channels to collect the scattered neutrons. For low temperature and high-field measurements, the sample was mounted at the end of the dilution fridge stick, with a base temperature of 50 mK, in a 11.5 T magnet. Muon spin relaxation ( $\mu$ SR)

\*leland.harriger@nist.gov

†singhdk@missouri.edu

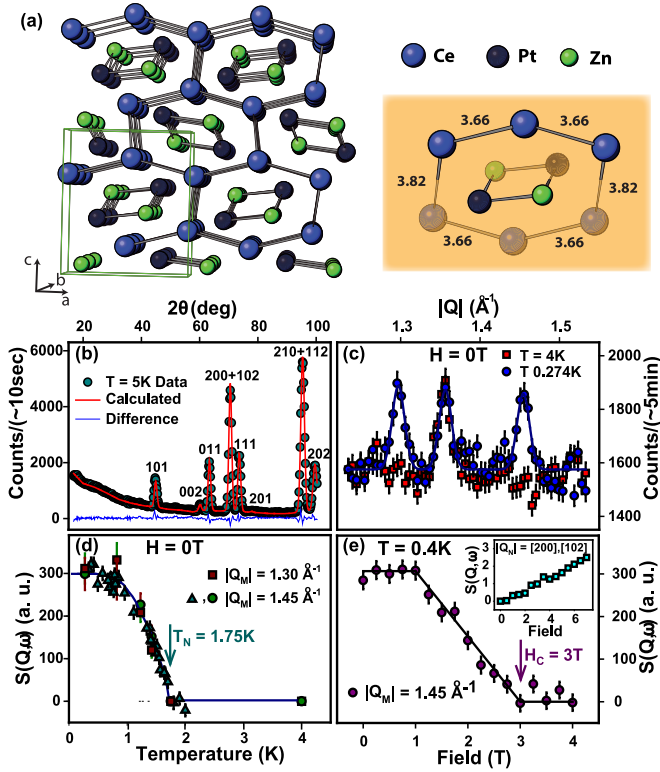


FIG. 1. Crystal structure and elastic neutron scattering measurement of CePtZn. (a) Crystal structure of CePtZn. (b) Powder neutron diffraction confirms the high quality of the powder. (c) The resolution limited elastic peaks are found to develop at low temperature in the elastic scan, indicating long-range magnetic order in the system. (d) Magnetic order parameter as a function of temperature is plotted in this figure. Fitting of the order parameter using a power law yields a Neel temperature of  $T_N = 1.75$  K. (e) Plot of an elastic peak intensity, at  $Q = 1.45 \text{ \AA}^{-1}$ , as a function of field shows that the magnetic order disappears at  $H_c = 3$  T. The inset shows a weak enhancement in the nuclear peak position as a function of field. It arises due to the alignment of the uncorrelated Ce ions to the applied field direction, as the field strength increases.

measurements were performed on 500 mg of CePtZn on the EMU spectrometer at the ISIS-Rutherford Appleton Labs.

In Fig. 1(c), we plot the elastic data obtained on SPINS. Resolution limited magnetic peaks that are incommensurate with respect to nuclear peaks are found to develop as the sample is cooled below  $T = 1.75$  K, indicating the development of long-range magnetic order in the system. The temperature dependence of the magnetic peak is illustrated in Fig. 1(d). The order parameter versus temperature plot is fitted with a power-law expression, suggesting a second-order phase transition to the long-range ordered state in CePtZn. Neutron scattering measurements point to the presence of incommensurate magnetic order in CePtZn, which is also complemented by  $\mu$ SR measurements (as discussed below).

$\mu$ SR results are plotted in Fig. 2(a). The time-dependent decay asymmetry is described by a strongly damped oscillatory function indicative of a long-range ordered state. The experimental data is well described by the following equation:

$$A(t) = A_s e^{-\lambda_s t} J_0(\gamma_\mu B_{\max} t) + A_d e^{-\lambda_d t} + A_{bkg}, \quad (1)$$

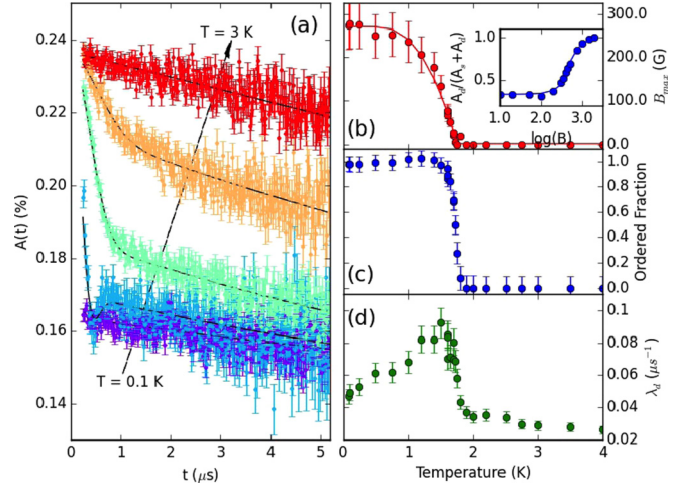


FIG. 2.  $\mu$ SR measurements of CePtZn. (a) Time-dependent asymmetry for selected temperatures between 0.1 and 3 K. The solid lines are fits of the data using Eq. (1). (b) Temperature dependence of  $B_{\max}$  extracted from fit. Inset shows the external field dependence of the initial asymmetry. (c) Fraction of the sample in the magnetically ordered state as a function of temperature. (d) Dynamic or longitudinal depolarization as a function of temperature.

where  $J_0$  is the Bessel function of the first kind,  $\gamma_\mu B_{\max}$  is the internal field distribution,  $\gamma_\mu/2\pi = 0.0135$  MHz/G is the muon gyromagnetic ratio,  $\lambda_s$  is the additional damping of the oscillatory component from the static field,  $\lambda_d$  the longitudinal or “dynamic” component, and  $A_{Bkg}$  is the constant background contribution from muons not stopping in the sample. The observation of a Bessel function with phase shift demonstrates that the magnetic structure is incommensurate such that there is a periodic modulation of the static magnetic field between muon stopping sites. This result is consistent with our elastic neutron scattering data [Fig. 1(c)], where  $Q$  values of magnetic Bragg peaks do not index to the commensurate superlattice positions of the unit cell. As shown in Fig. 2(b),  $B_{\max}$  follows the temperature dependence of the order parameter under the mean-field approximation, with a transition temperature of  $T_N = 1.75(2)$  K and the maximum local field of 270(25) G. The volume fraction of the ordered state shown in Fig. 2(c) sharply increases at  $T_N$ , as such revealing a single well defined transition temperature and uniform magnetic ordering across the sample. Lastly, the longitudinal relaxation, sensitive to the low-energy dynamics of the system, is shown in Fig. 2(d) where again a sharp upturn near  $T_N$  is observed. This is possibly attributed to the critical scattering at the phase transition.

$\mu$ SR measurements complement the previous electrical and magnetic measurements where a critical phase was inferred to exist after the disappearance of long-range ordered state [10]. As shown in Fig. 1(e), the long-range magnetic order indeed disappears at a critical field of  $H_c = 3$  T, which is smaller than that estimated from magnetic and electrical measurements in Ref. [10]. The inset in Fig. 1(e) shows a weak enhancement in the nuclear peak position as a function of field. Not all Ce ions participate in the correlated moment formation. The uncorrelated ions tend to align along the field as the field strength increases. Next, we investigate whether

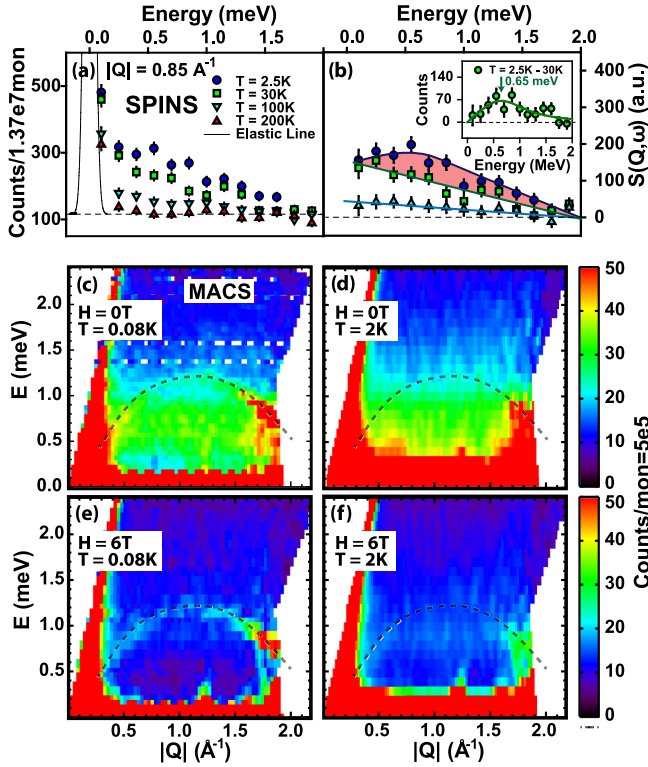


FIG. 3. Inelastic neutron scattering data as a function of temperature. (a) and (b) Energy scans at fixed  $Q$  and at different temperatures are shown in this figure. A peak-type structure, centered at  $E = 0.65$  meV, tends to develop as temperature is reduced. Inelastic spectra is fitted using damped harmonic oscillator model (see text). The inset illustrates the development of the gapped excitation below  $T \simeq 30$  K. (c) and (d) Momentum-energy ( $Q$ - $E$ ) color map, at two temperatures of  $T = 80$  mK and 2 K, respectively, depicting the  $Q$ -independent nature of the inelastic excitation across the magnetic order transition temperature. The gap seems to be independent of the development of long-range magnetic order. The dashed line highlights the scattering from helium roton excitation. (e) and (f)  $Q$ - $E$  maps at  $T = 80$  mK and 2 K at  $H = 6$  T, respectively. Clearly, the application of magnetic field significantly suppresses inelastic excitation.

the spectral weight associated with the elastic peaks transfer into dynamic correlations when the static order disappears. Much to our surprise, interesting new properties are discovered in inelastic neutron scattering measurements. As shown in Figs. 3(a) and 3(b), an excitation peaking at  $E = 0.65$  meV is detected in SPINS measurement. At first, it seems that the inelastic spectra consists of a gapped excitation and a quasielastic peak. But we were unable to separate them statistically. Plots of  $\chi''$  versus  $E$  in Figs. 4(e) and 4(f) (discussed below) do not support the presence of quasi-elastic behavior either. The gap co-exists with long-range magnetic order. Although the gap becomes more pronounced as the measurement temperature decreases—suggesting its magnetic characteristic, distinguishable spectral weight (with respect to the background) is observed at temperature as high as  $T = 100$  K. Furthermore, the gap is found to be wave-vector independent, as shown in Fig. 3(c) of MACS measurements. The intensity of the  $Q$ -independent gap does not seem to be much affected across the magnetic order transition at

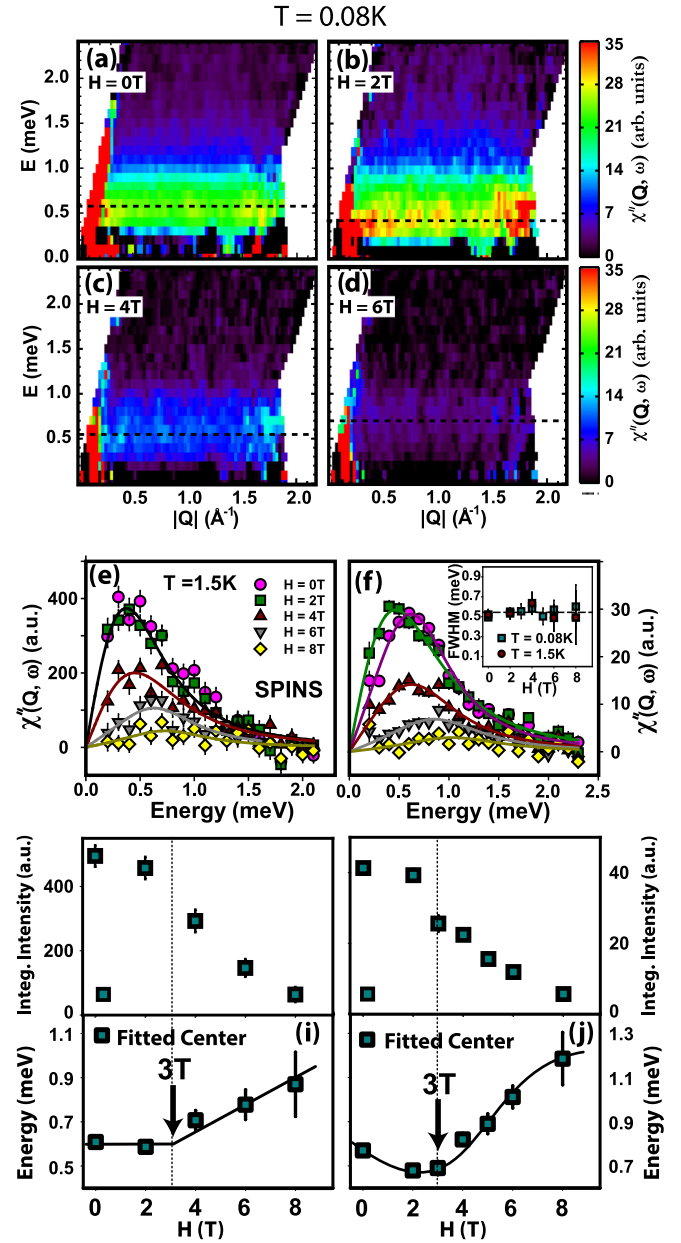


FIG. 4. Inelastic measurements in applied magnetic field. (a)–(d)  $Q$ - $E$  maps at different magnetic field application of  $H = 0, 2, 4,$  and  $6$  T at  $T = 80$  mK, respectively. Remnants of gapped excitation can still be seen at  $H = 4$  T and  $6$  T, which is larger than the critical field to suppress the long-range order. (e) and (f) Plots of dynamic susceptibility as a function of energy at different fields and at  $T = 1.5$  K and  $80$  mK, respectively.  $\chi''$  was deduced from the high-resolution fixed- $Q$  scans on SPINS at final neutron energy of  $E_f = 2.5$  meV. Inelastic data are well described by the damped harmonic oscillator model (see text). The excitation persists to a high field of  $H = 8$  T. At  $H = 9$  T, the excitation is completely suppressed. Inset [in (f)] shows the plot of estimated linewidth, FWHM, of the gapped excitation as a function of field. The linewidth of the excitation remains field-independent. (g) and (h) Integrated intensity vs applied magnetic field at  $T = 1.5$  K and  $80$  mK, respectively, are plotted. (i) and (j) In this plot, we show the field dependence of the center of the excitation as a function of field at  $T = 1.5$  K and  $80$  mK, respectively. A dramatic change in the peak position of the excitation around the critical field value,  $H_c = 3$  T, is observed at low temperature.

$T = 1.75$  K, Fig. 3(d). However, the magnetic field application clearly tends to suppress the gapped excitation, as shown in Figs. 3(e) and 3(f).

Both the  $Q$ -independent characteristic and the finite intensity at high temperature of magnetic gap suggest the crystal-field nature, more specifically the excited state of the ground-state doublet, of the excitation. Previous work on the isostructural dense Kondo lattice, CePtSn, showed that the crystal-field (CEF) level scheme consists of a doublet ground state and three excited states, described by the superpositions of  $|\pm 1/2\rangle$ ,  $|\pm 3/2\rangle$ , and  $|\pm 5/2\rangle$  states [11]. Similar CEF level scheme can be expected in CePtZn, as both compounds are isoelectronic in nature. There are some anomalies, however, that need to be addressed. First, the width of the inelastic peak [Figs. 3(a)–3(d)] is much broader than the instrument resolution, which is atypical of the resolution-limited crystal-field excitations. Second, the excitation seems to be suppressed by magnetic field application [17]. Therefore some other mechanism in addition to the CEF excitation, may be playing an important role in the evolution of magnetic gap.

Further information behind the magnetic gap formation is obtained by performing inelastic neutron scattering measurements in applied magnetic field. Inelastic neutron data in applied field are plotted in Figs. 4(a)–4(d). It is immediately noticed that the  $Q$ -independent excitation strongly weakens as the applied field is increased to  $H = 6$  T. Weak remnants of the excitation are still visible in Fig. 4(d). We have performed high resolution inelastic measurements on SPINS spectrometer to get quantitative information. At the final neutron energy of  $E_f = 2.5$  meV, the spectrometer's resolution is narrowed down to  $\Delta E = 80$   $\mu$ eV. Figures 4(e) and 4(f) show the high-resolution measurements data at different magnetic fields and collected at two different temperatures of  $T = 1.5$  K and 80 mK. We find that (a) the inelastic excitation fully develops into a peak-type structure as temperature is reduced to  $T = 80$  mK, and (b) magnetic excitation is fully suppressed as the applied magnetic field is increased above  $H = 8$  T.

Under the single-ion formulation, an applied magnetic field tends to affect the crystal-field excitation via the following modification to the CEF Hamiltonian [11,18]:

$$H = H_{\text{CEF}} - g_J \mu_B \mathbf{B} \cdot \mathbf{J}, \quad (2)$$

where  $g_J$  is the Lande factor and  $J$  is the total angular momentum. The net field  $\mathbf{B}$  is a combination of the applied field, the dipolar interaction, and the exchange interaction of  $\text{Ce}^{3+}$  ion with its neighbors. While detail calculations are needed to estimate the exact value of  $\mathbf{B}$  and, hence, the strength of the field term in the single-ion Hamiltonian, the field application will cause a rearrangement of the excited states. At the same time, the single-ion Hamiltonian provides a more accurate description of the excitation that is much larger than  $T_N$  and  $T_K$ , measures of the exchange and the coherence interactions, respectively. In CePtZn, the excitation ( $E = 0.65$  meV or 7 K) is comparable to both quantities,  $T_N = 1.75$  K and the Kondo temperature  $T_K \simeq 4.7$  K [10]. Therefore single-ion Hamiltonian cannot be solely responsible for the unusual field dependence of the excitation.

The dynamic susceptibility  $\chi(Q, \omega)$ , deduced from the inelastic data using the relation:  $S(Q, \omega) = (1/\pi)\chi''/(1 - e^{-E/k_B T})$ , are plotted in Figs. 4(e) and 4(f). The thermally

balanced dynamic susceptibility data are found to be best described by the damped harmonic oscillator model, given by

$$S(Q, \omega) = A_0 + A \frac{\Gamma E E_0}{(E^2 - E_0^2)^2 + 4(\Gamma E)^2}, \quad (3)$$

where  $\Gamma$  is the linewidth and  $A$  is the integrated intensity of the peak. The fitted values of  $\Gamma$ , FWHM, at  $T = 1.5$  K and 80 mK are plotted as a function of field in the inset of Fig. 4(f). Although, the linewidth is much broader than the instrument resolution ( $\simeq 80$   $\mu$ eV), it remains independent of field both above and below the magnetic order transition temperature,  $T_N = 1.75$  K. Also, the values of FWHM at both temperatures are comparable. In general, a temperature independent broad linewidth suggests the occurrence of the valence fluctuation in a heavy fermion system [1]. In Figs. 4(g)–4(j), we have plotted the field dependencies of the integrated intensity and the center of the gapped excitation at  $T = 1.5$  K and 80 mK, respectively. Although, the peak of the excitation appears to shift to the higher energy at both temperatures, a discernible change around the critical field value of  $H_c = 3$  T is clearly observable. At  $T = 80$  mK, the peak position first shifts towards lower energy, as if the excitation is tending to merge to the quasielastic line and thus develop a short-range dynamic structure, before shifting to higher energy as the applied field is increased. Such a dramatic field dependence of the gapped excitation is apparently arising due to the competing interaction between the crystal-field excitation and a possible quantum critical state. The integrated intensity is also found to decrease significantly as the system crosses the critical field regime. Similar observations were previously associated to the quantum critical state in heavy fermion systems [9,19,20]. Since the gapped excitation is  $Q$ -independent, any such critical state would be primarily dominated by local Kondo interaction. While more research is needed to verify the field-induced quantum critical nature of CePtZn, the unusual field dependencies of  $\Gamma$  and gap excitation energy indicate that some other mechanism (in addition to the crystal-field excitation) plays important role in the gap formation.

In summary, we have presented detailed neutron scattering and muon spin relaxation measurements of dense Kondo lattice CePtZn. Our experimental investigations reveal the presence of long-range incommensurate magnetic order with a transition temperature of  $T_N = 1.75$  K. In a surprising observation, the long-range order is found to exist with a  $Q$ -independent gapped excitation. Although many properties of the gapped excitation can be explained under the ambit of the crystal-field level scheme, the unusually broad linewidth of the excitation and its field dependencies are anomalous. A qualitative interpretation of the inelastic data in field suggests the presence of local quantum critical behavior as previously anticipated based on the electrical and magnetic measurements [10], co-existing with the crystal-field excitation. Future theoretical and experimental researches, especially on the single crystal specimen, are very desirable to further understand these intriguing properties.

D.K.S. thankfully acknowledges the support by the Department of Energy, Office of Science, Office of Basic Energy

Sciences under the Grant No. DE-SC0014461. This work utilized facilities supported in part by the National Science

Foundation under Agreement No. DMR-1508249 and the Department of Commerce.

- 
- [1] A. C. Hewson, *The Kondo problem to Heavy Fermions* (Cambridge University Press, Cambridge, 1993).
- [2] Z. Fisk, D. Hess, C. Pethick, D. Pines, J. Smith, J. D. Thompson, and J. Willis, *Science* **239**, 33 (1988).
- [3] P. Coleman and A. Schofield, *Nature (London)* **433**, 226 (2005).
- [4] S. Sachdev, *Quantum Phase Transitions* (Cambridge University Press, New York, 1999).
- [5] Q. Si, S. Rabello, K. Ingersent, and J. Smith, *Nature (London)* **413**, 804 (2001).
- [6] A. Schroder, G. Aeppli, R. Coldea, M. Adams, O. Stockert, H. V. Lhneysen, E. Bucher, R. Ramazashvili, and P. Coleman, *Nature (London)* **407**, 351 (2000).
- [7] J. Custers, P. Gegenwart, H. Wilhelm, K. Neumaier, Y. Tokiwa, O. Trovarelli, C. Geibel, F. Steglich, C. Pepin, and P. Coleman, *Nature (London)* **424**, 524 (2003).
- [8] L. S. Wu, M. S. Kim, K. Park, A. M. Tsvelik, and M. C. Aronson, *Proc. Natl. Acad. Sci. USA* **111**, 14088 (2014).
- [9] P. Gegenwart, Q. Si, and F. Steglich, *Nat. Phys.* **4**, 186 (2008).
- [10] S. K. Dhar, R. Kulkarni, H. Hidaka, Y. Toda, H. Kotegawa, T. Kobayashi, P. Manfrinetti, and A. Provino, *J. Phys. Condens. Matter* **21**, 156001 (2009).
- [11] M. Divis, H. Nakotte, F. de Boer, P. de Chatel, and V. Sechovsky, *J. Phys. Condens. Matter* **6**, 6895 (1994).
- [12] J. Sakurai, Y. Yamaguchi, S. Nishigori, T. Suzuki, and T. Fujita, *J. Magn. Magn. Mater.* **90–91**, 422 (1990).
- [13] T. Takabatake and H. Fujii, *Jap. J. Appl. Phys. Ser. 8*, 254 (1993).
- [14] S. K. Malik, D. T. Adroja, S. K. Dhar, R. Vijayaraghavan, and B. D. Padalia, *Phys. Rev. B* **40**, 2414 (1989).
- [15] H. Kadowaki, T. Ekino, H. Iwasaki, T. Takabatake, H. Fujii, and J. Sakurai, *J. Phys. Soc. Jpn.* **62**, 4426 (1993).
- [16] S. K. Dhar, R. Kulkarni, P. Manfrinetti, M. Pani, Y. Yonezawa, and Y. Aoki, *Phys. Rev. B* **76**, 054411 (2007).
- [17] I. Mirebeau, P. Bonville, and M. Hennion, *Phys. Rev. B* **76**, 184436 (2007).
- [18] T. Saso and T. Kasuya, *Theory of Valence Fluctuation State and Heavy Fermion Systems* (Springer, Berlin, (1985).
- [19] D. K. Singh, A. Thamizhavel, J. W. Lynn, S. Dhar, J. Rodriguez-Rivera, and T. Herman, *Sci. Rep.* **1**, 117 (2011).
- [20] J. X. Zhu, D. R. Grempel, and Q. Si, *Phys. Rev. Lett.* **91**, 156404 (2003).